Acta Crystallographica Section D

Volume 70 (2014)

Supporting information for article:

Crystal structures of inactive CRP species reveal the atomic details of allosteric transition that discriminates cyclic nucleotide second messengers

Seung-Hyeon Seok, Hookang Im, Hyung-Sik Won, Min-Duk Seo, Yoo-Sup Lee, Hye-Jin Yoon, Min-Jeong Cha, Jin-Young Park and Bong-Jin Lee

Supporting Information

S1. Structural and functional relevance of CDD dimerization

Some CRP-family proteins that resemble the cAMP-bound CRP with dissociated CDD conformations exert an inherent activity without effector molecules (Altenhofen *et al.*, 1991; Bernlohr *et al.*, 1974; Eiting *et al.*, 2005). Conversely, the dimerized CDDs can be a characteristic of inactive CRP species. The CDD dimerization in the inactive, apo-state has been first suggested for the CRP-family protein CooA (Lanzilotta *et al.*, 2000; Chan, 2000; Komori *et al.*, 2007; Borjigin *et al.*, 2007). Despite the observed CDD dissociation that exhibits a profound asymmetry, which is likely due to severe crystal packing forces, its solution structure was theoretically modeled to be dimerized via the αDs (Chan, 2000). Subsequently, another CRP-family protein, CprK, demonstrated a valid CDD dimerization that is specific to its off-state (Joyce *et al.*, 2006). Finally, the compact dimerization of the CDDs that results in the inward positioning of the αFs was observed in D138L-CRP and the low-resolution apo-CRP crystal structures (Sharma *et al.*, 2009), which is corroborated by the present apo-CRP and cGMP-CRP structures (Fig. 1*a*).

In contrast to the present crystal structure, the previous NMR structure of apo-CRP that was determined by Popovych *et al.* (Popovych *et al.*, 2009) is puzzling as it revealed dissociated CDDs that exhibited the shorter-length αDs and the protrusion of the αFs onto the top surface. Additionally, crystal structures of the apo-CRP from *Mycobacterium tuberculosis* (*Mtb*-apo-CRP) (Kumar *et al.*, 2010; Reddy *et al.*, 2009; Gallagher *et al.*, 2009) closely resembled the NMR structure of the *E. coli* apo-CRP (*Ec*-apo-CRP) with the dissociated CDDs. Based on the present insights into CRP allostery, the observed CDD dissociation in the *Mtb*-apo-CRP crystal structure is fully attributable to significant sequence variations from our *Ec*-apo-CRP crystal structure. First, L137 in *Ec*-CRP corresponds to T144 in *Mtb*-CRP (Supplementary Fig. S4*b*). Because the hydrophobic L137, together with L134, plays a critical role in CDD dimerization of the apo-form (Fig. 2*a*), its mutation to the polar threonine could trigger CDD dissociation. This possibility is supported by a similar A144T mutation of *Ec*-CRP

that results in the formation of the constitutively active CRP* mutant (Won *et al.*, 2009; Harman, 2001; Passner *et al.*, 2000), implying CDD dissociation through the substitution of A144 at the hydrophobic interface of the CDD dimer (Fig. 2*a*) with threonine. Moreover, *Ec*-apo-CRP and *Mtb*-apo-CRP possess significant sequence variations particularly in the flap region (Supplementary Fig. S4*b*). First, the stabilization of the dimerized CDD orientation by the flap residue E54 in *Ec*-apo-CRP, which directly interacts with R185 in αF (Fig. 4*a*), is not possible in *Mtb*-apo-CRP, in which the corresponding residue is proline. Similarly, the interdomain hydrophobic interaction between M59 (N67 in *Mtb*-apo-CRP) and L195 (W203 in *Mtb*-apo-CRP) in *Ec*-apo-CRP (Fig. 3*b*) is not expected for the polar asparagine at the equivalent position of *Mtb*-apo-CRP. Conversely, the positively charged flap residues K54 and K56 of *Mtb*-apo-CRP, which stabilize the dissociated CDDs by charge interactions with D174 (K166 in *Ec*-CRP) and E179 (E171 in *Ec*-apo-CRP), respectively, are replaced by S46 and A48, respectively, in *Ec*-apo-CRP. Similarly, the side chain of R59 in *Mtb*-apo-CRP, which forms a salt bridge with D140 (N133 in *Ec*-apo-CRP) in the opposite subunit to position the flap close to the hinge, is mutated to an isoleucine in *Ec*-apo-CRP, in which this flap movement is not induced. Collectively, the sequence variations between *Ec*- and *Mtb*-apo-CRP appear to have been specifically adapted for the stabilization of the dimerized CDDs in *Ec*-apo-CRP and the dissociated CDDs in *Mtb*-apo-CRP. Therefore, the observation of dissociated CDDs in the NMR structure of *Ec*-apo-CRP (Popovych *et al.*, 2009) may also be attributable to mutations and/or spin labeling, as discussed by Sharma *et al* (Sharma *et al.*, 2009), which were introduced for paramagnetic relaxation enhancement experiments to obtain long-range distance restraints. In particular, modifications at the flap (K57 and Q66), αE (Q170) and/or the C-terminal β11 (S197) residues may have caused similar domain alterations that dissociate the CDDs, as induced in *Mtb*-apo-CRP. The intermediate conformations of CRP-family proteins (Won *et al.*, 2009), which have been observed for CooA (Komori *et al.*, 2007), CprK (Lanziotta *et al.*, 2000), and PrfA (Eiting *et al.*, 2005), wherein the αFs are positioned in a manner that is incompatible with DNA binding despite the dissociated CDDs, also support the concept that CRP can adopt an alternatively inactive conformation even with CDD dissociation, with minor structural changes at certain positions.

S2. Conformational asymmetry of apo-CRP in solution

The asymmetry of the domain orientations between subunits was consistently observed in nearly all of the CRP-related crystal structures, including CRP-family proteins and CRP orthologues (Won *et al.*, 2009; Kumar *et al.*, 2010; Reddy *et al.*, 2009; Gallagher *et al.*, 2009). Even in the cAMP-CRP structure, the asymmetry is observed, although it is very subtle relative to the apo-CRP structure (Passner *et al.*, 2000; Weber & Steitz, 1987). Conversely, NMR and molecular dynamics simulations indicated no detectable asymmetry in solution, and, therefore, the observed asymmetries have been often regarded as an artifact due to crystal packing forces (Won *et al.*, 2009; Chan, 2000). However, an alternative model can be derived from the present examination of the heterogeneous conformations of the known structures. The present apo-CRP, the previous D138L-CRP (PDB ID: 3FWE), and the three dimers of low-resolution apo-CRP structures (PDB ID: 3HIF) slightly differ from one another in the orientations of the CDD pairs with respect to the NNDs. Additionally, the interdomain interactions between the CDDs and NNDs are sparse (Fig. 4*a*) and organized differently among these crystal structures and between subunits of individual dimers. Thus, the suggestion by Sharma *et al.* (Sharma *et al.*, 2009) could be reasonable that the pairs of CDDs are mobile as one rigid body about the hinge, *i.e.*, that the CDD orientations are not firmly maintained, and their interdomain interactions with the NNDs would be transiently formed or dynamically equilibrated in solution. These heterogeneities in the CDD orientations are primarily attributable to the different geometries of the interdomain hinge regions (V126-N133) that extend from αC. The hinge conformations in inactive CRP species, including the NMR and crystal structures of apo-CRP and the crystal structures of D138L-CRP and cGMP-CRP, are variable between individual subunits and are hardly stabilized as a regular α-helix but include irregular folds such as an extended stretch, a short 3_{10}-helix, or a helical loop (Supplementary Fig. S1*b*). Hence, the observed heterogeneity in the hinge conformation, which is also supported by its flexible nature (Popovych *et al.*, 2006, 2009; Tomlinson *et al.*, 2006; Lanzilotta *et al.*, 2000), suggests that in solution, the individual hinge regions of an apo-CRP dimer may be sampling a rapid equilibrium between diverse folded and disordered states with interconverting CDD

orientations. The fact that no significant interhinge interactions that stabilize their asymmetric folds are observed also supports the independent dynamic properties of individual hinges in the apo-CRP dimer. The heterogeneous folds of the hinge are also explicit for an inherent helical propensity that contributes to the cAMP-induced helical stabilization of the region, which was first suggested from our previous NMR study (Won *et al.*, 2000). Agonist-induced helical transitions in αC have been recently reported for other cAMP-regulated proteins, such as cNMP-dependent ion channels (Altieri *et al.*, 2008; Clayton *et al.*, 2004; Schünke *et al.*, 2011; Puljung & Zagotta, 2013). In particular, a collection of apo-state crystal structures of the prokaryotic, cNMP-activated K^+ channel MloK1 revealed diverse conformations in the C-terminal region of αC (Altieri *et al.*, 2008), although these were not detected in the NMR structure (Schünke *et al.*, 2011). Moreover, the region stably folded into an α-helix in the cNMP-bound states (Altieri *et al.*, 2008; Clayton *et al.*, 2004). Collectively, we finally suggest that apo-CRP in solution would be under a rapid conformational equilibrium that generates an ensemble of asymmetric (open and closed) domain orientations due to the dynamic and heterogeneous folds of the hinge regions. Regardless of the asymmetry or conformational exchange, both subunits are involved in the inactive state, as the αFs are inwardly positioned in a manner that is incompatible with DNA binding.

Supplementary References

Borjigin, M., Li, H., Lanz, N. D., Kerby, R. L., Roberts, G. P. & Poulos, T. L. (2007). *Acta Cryst.* **D63**, 282-287.

Joyce, M. G., Levy, C., Gábor, K., Pop, S. M., Biehl, B. D., Doukov, T. I., Ryter, J. M., Mazon, H., Smidt, H., van den Heuvel, R. H., Ragsdale, S. W., van der Oost, J. & Leys, D. (2006). *J. Biol. Chem.* **281**, 28318-28325.

Komori, H., Inagaki, S., Yoshioka, S., Aono, S. & Higuchi, Y. (2007). *J. Mol. Biol.* **367**, 864-871.

Schrodinger, LLC (2010). The PyMOL Molecular Graphics System, Version 0.99rc6.

Mills J. E. and Dean P. M. (1996). *J Comput Aided Mol Des*. **10(6)**, 607-22

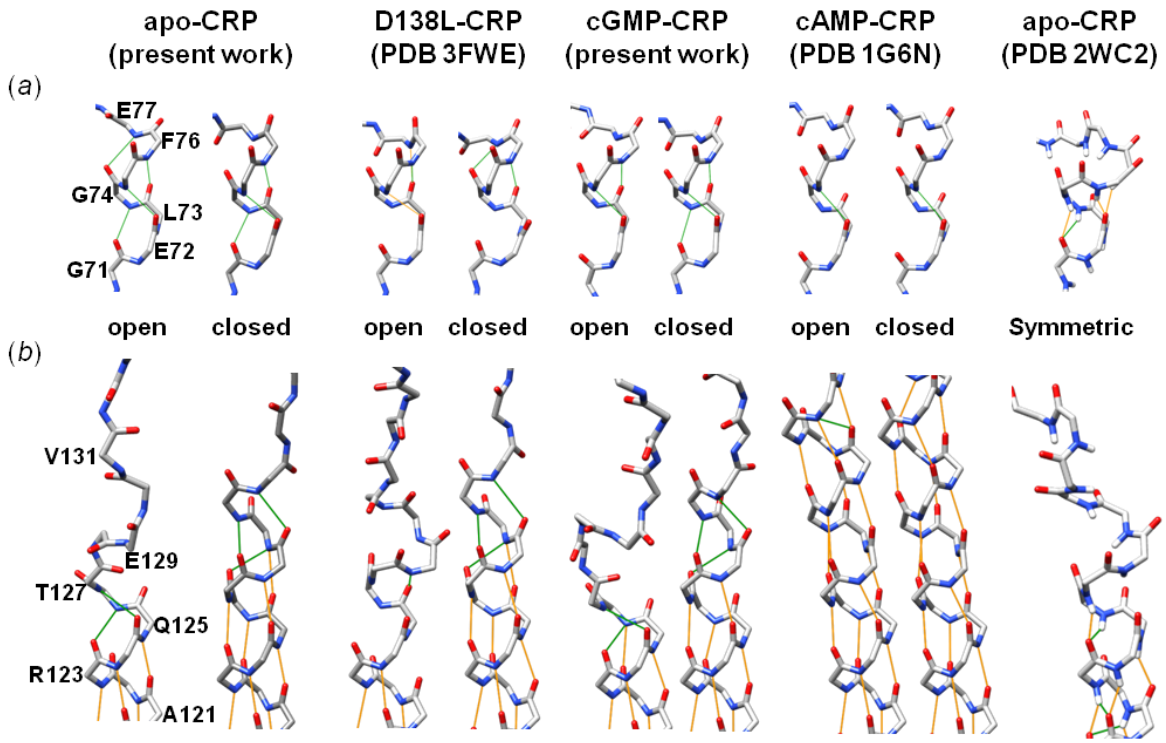

Figure S1 Backbone hydrogen bonding patterns of the ηN (*a*) and αC (*b*) helices observed in various states of CRP. The C^{α} positions are labeled with the corresponding residues in the leftmost panels, and the other structures are shown from the same N-terminus (G71 in the upper panels and A121 in the bottom panels). Hydrogen bonds are depicted as green lines for CO(i)-HN(i+3) and orange lines for CO(i)-HN(i+4) hydrogen bonds. Hydrogen bonds were identified using the FindHbond tool of the UCSF Chimera program (Pettersen *et al.*, 2004).

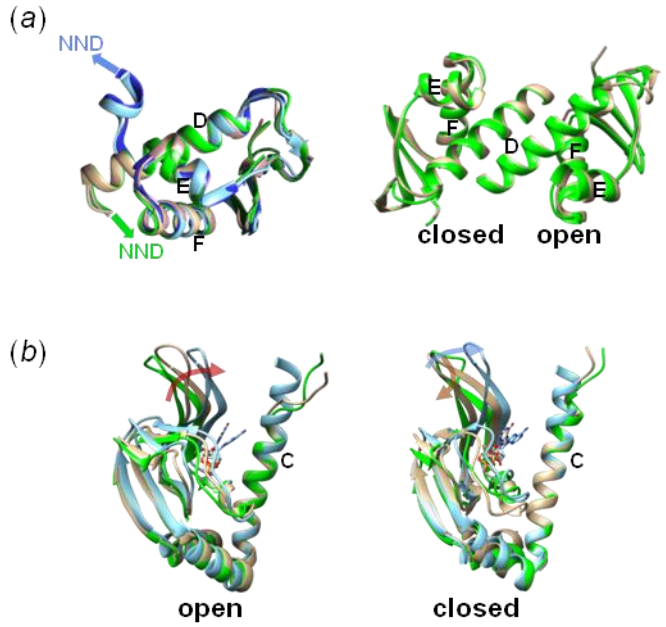

Figure S2 Structural comparison of individual domains. Ribbon representations of apo-CRP, cAMP-CRP, and cGMP-CRP that are colored green, sky blue, and tan, respectively. The C-, D-, E-, and F-helices are labeled with the corresponding letters. (*a*) In the left panel, all of the individual CDDs in the three CRP structures are superposed. The CDDs in the closed subunits are colored forest green, cornflower blue, and orchid for apo-CRP, cAMP-CRP, and cGMP-CRP, respectively. The N-terminal connection to the NND is indicated by a green arrow for apo- and cGMP-CRP and a cornflower-blue arrow for cAMP-CRP. In the right panel, CDD dimers of apo- and cGMP-CRP upon superposition of equivalent C^{α} atoms in the CDDs of the closed subunit. (*b*) Individual NNDs of the open and closed subunit in the three CRP structures upon superposition of equivalent C^{α} atoms in the αCs (D111-V126). cNMPs are shown as sticks. The flap movements upon cNMP binding are indicated by arrows.

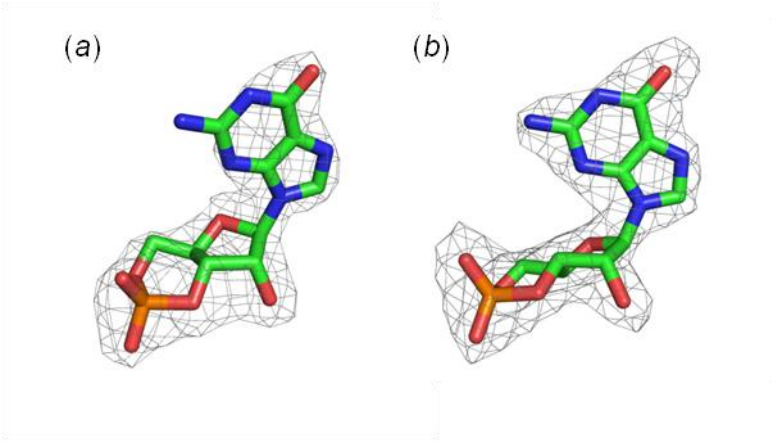

Figure S3 The F_o - F_c omit maps (grey; contoured at 3.0 Å) showing the electron densities of bound cGMPs at open (*a*) and closed (*b*) subunits. The stick presentations of cGMPs are coloured green for carbon, blue for nitrogen, red for oxygen and orange for phosphorus atoms. This figure was generated using the PyMOL program (Schrodinger, 2010).

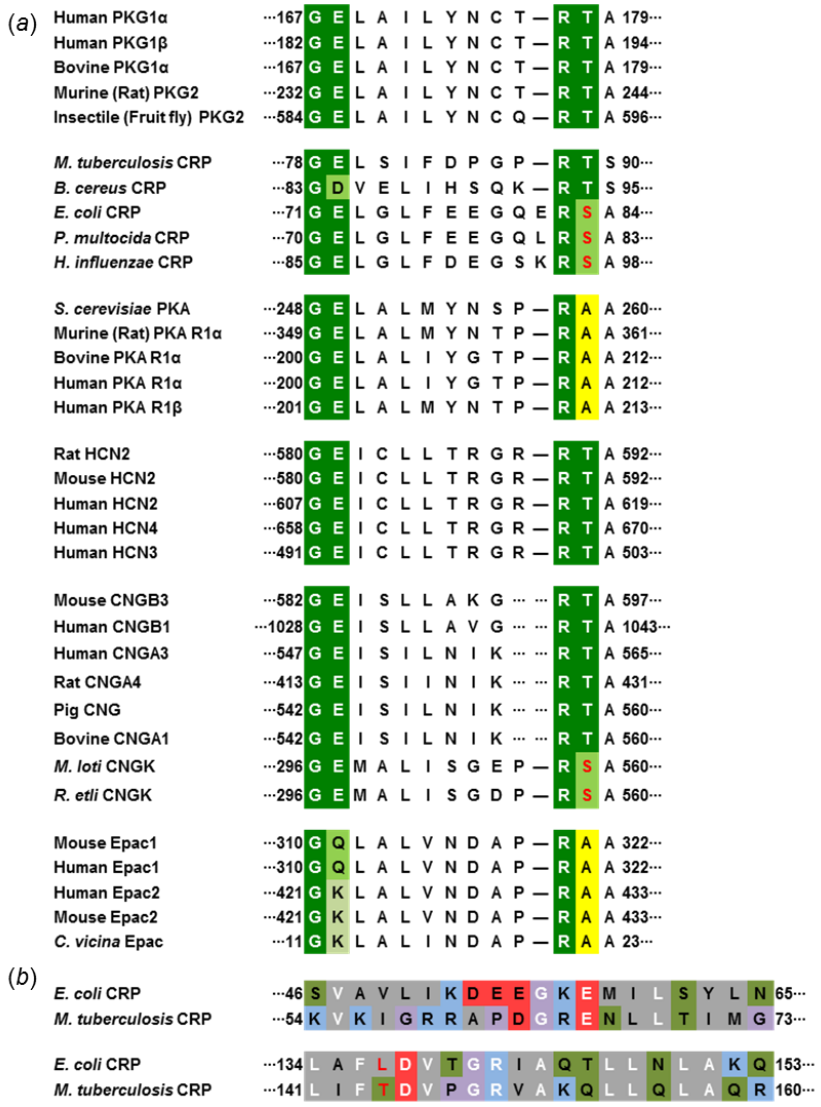

Figure S4 Sequence comparison of CRP with other cNMP-regulated proteins. (*a*) A portion of the cNMP-binding β-roll sequence is aligned to show the positional conservation of the residues that interact with cNMP, which are highlighted by colored boxes. (*b*) Amino acid sequences of *E. coli* CRP and *M. tuberculosis* CRP are aligned at the flap (upper panel) and αD (bottom panel) regions. Strictly conserved residues are indicated by white letters. The box color indicates the charge (red and blue for negative and positive, respectively), polarity (green and orchid for polar and neutral, respectively) and hydrophobicity (gray) of each residue.

Supplementary Fig. S5

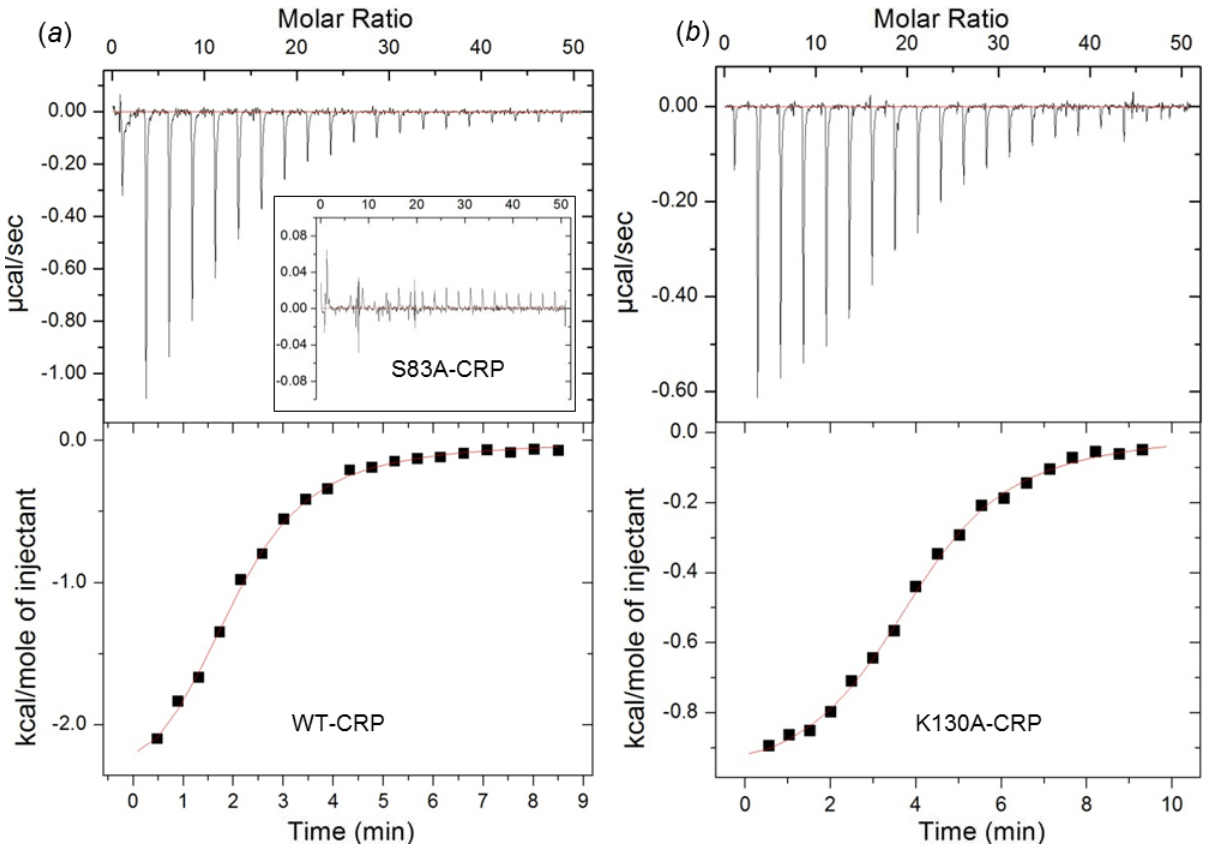

Figure S5 ITC analysis of cGMP binding to wild-type CRP (*a*), S83A-CRP (inset in *a*), and K130A-CRP (*b*). Upper panel presents thermogram obtained during the titration and lower panel shows the corresponding binding isotherm, where each point (2 µl injection) represents the integrated heat of the associated peak in the thermogram. The first point (0.4 µl injection) was eliminated prior to the curve fitting.